

Synthesis, Characterization and Electrochemical Performance of Cobalt Oxides for Supercapacitor

Xiyang Yan, Yansu Wang*, Zhiling Ma*

College of Chemistry and Environmental Science, Hebei University, National Demonstration Center for Experimental Chemistry Education, Key Laboratory of Analytical Science and Technology of Hebei Province, Baoding 071002, China.

*E-mail: 15131200232@163.com, mazhiling838838@163.com

Received: 28 September 2017 / Accepted: 26 November 2017 / Published: 16 December 2017

Cobalt oxides were prepared by calcinating the precursor which precipitated from $\text{Co}(\text{NO}_3)_2 \cdot 6\text{H}_2\text{O}$ at pH=10.08, 9.90, 9.75, 9.64 $\text{NH}_3\text{-NH}_4^+$ buffer solution. XRD, XPS and SEM analysis proved that all of the samples were Co_3O_4 and CoO mixing with honeycomb-like morphology. High buffer pH acted as conducive solution when $\text{Co}(\text{II})$ convert to $\text{Co}(\text{III})$. Electrochemical performance test indicated that the high $\text{Co}(\text{III})$ content is excellent for the electrochemical performance. But when the pH of the buffer is high, it is not conducive to the uniform distribution of sample particles, which can affect its electrochemical performance. So at the buffer pH 9.90, a higher $\text{Co}(\text{III})$ with excellent uniform degree cobalt oxides was obtained and exhibited best electrochemical performance. And when the current density of $1 \text{ A} \cdot \text{g}^{-1}$, the specific capacitance up to $726 \text{ F} \cdot \text{g}^{-1}$.

Keywords: Cobalt oxides; Preparation pH; Supercapacitor; Electrochemical properties

1. INTRODUCTION

As an energy storage device, supercapacitor has been considered to be the most promising equipment in recent years [1,2] The device can be classified into two categories including electrical double layer capacitor (EDLCs) and pseudo capacitor. Transition metal oxides [3] are good choices for pseudo capacitors because they can store more energy and be charged through the Faraday reaction. So far, various metal oxide materials such as MnO_2 [4], V_2O_5 [5], Co_3O_4 [6], Fe_3O_4 [7,8], and NiO [9,10] have been widely used in electrode materials. Recently, the interest of Co_3O_4 as electrode materials for pseudo capacitors is increasing due to its high theoretical capacitance (up to $3650 \text{ F} \cdot \text{g}^{-1}$), low cost and environmental friendly nature [11]. Qiu [12] prepared a nickel foam-supported shell-like Co_3O_4 array through the microwave hydrothermal method and the obtained material has an excellent specific

capacitance. Zhao [13] prepared the mesoporous Co_3O_4 material by in-situ synthesis template method and the material specific capacitance was $329 \text{ F}\cdot\text{g}^{-1}$. Through chemical precipitation and heat treatment, Fan [14] obtained 3D Co_3O_4 powder material assembled by ultra-thin nanosheet with specific capacitance of $896 \text{ F}\cdot\text{g}^{-1}$.

In general, the Co_3O_4 was prepared by using Co^{2+} salts as cobalt sources to obtain precursor such as cobalt oxalate [15] and $\text{Co}(\text{OH})_2$ [16] and followed by heat treatment. In this approach, the Co (II) was oxidized to Co (III) in the heat treatment process. In fact, for the oxidation degree, the difference between the sample surface and internal may lead to non-uniform products. Therefore, many researchers [17-20] improved the method by adding $\text{NH}_3\cdot\text{H}_2\text{O}$ into the solution of Co^{2+} salts to form $[\text{Co}(\text{NH}_3)_6]^{2+}$, which hope to convert Co^{2+} salts to $[\text{Co}(\text{NH}_3)_6]^{3+}$ easily, and Co (III) was obtained in the precursor formation process. However, when the $\text{NH}_3\cdot\text{H}_2\text{O}$ added, the concentration of NH_3 and OH^- will increase at the same time. The formation of $[\text{Co}(\text{NH}_3)_6]^{2+}$ and $\text{Co}(\text{OH})_2$ were competitive reactions in the system. The high concentration of OH^- will benefit to the $\text{Co}(\text{OH})_2$ formation and the Co (III) oxidation is difficultly in the solution. The high concentration of NH_3 is good for the formation of $[\text{Co}(\text{NH}_3)_6]^{2+}$ which converted to $[\text{Co}(\text{NH}_3)_6]^{3+}$ easily. If the $\text{NH}_3\cdot\text{H}_2\text{O}$ was added dropwise, the pH increased gradually and when pH increased to 7-8, $\text{Co}(\text{OH})_2$ was precipitated due to the pK_{sp} of $\text{Co}(\text{OH})_2$ is 14.23 [21]. Under this pH condition, NH_3 exists hardly as the pK_{b} of $\text{NH}_3\cdot\text{H}_2\text{O}$ is 4.75 [21]. If $\text{NH}_3\cdot\text{H}_2\text{O}$ was one-off pouring quickly, the $[\text{Co}(\text{NH}_3)_6]^{2+}$ and $\text{Co}(\text{OH})_2$ were generated simultaneously. However, a problem with this method is that the additional $\text{NH}_3\cdot\text{H}_2\text{O}$ leads to high concentration of NH_3 and OH^- in the solution which makes quickly formation of $[\text{Co}(\text{NH}_3)_6]^{2+}$ and $\text{Co}(\text{OH})_2$. Hence, variations formation occur in the precursor, and eventually makes reproducible results difficult to reobtain.

To obtained repeatable precursor, in this paper, cobalt nitrate was added to the high enough concentration of $\text{NH}_3\text{-NH}_4^+$ buffer solution, to ensure a stable concentration of NH_3 and OH^- . The affection of buffer pH on the morphologies and electrochemical performance of cobalt oxides were characterized by XRD, XPS, SEM and electrochemical performance test.

2. EXPERIMENTAL

2.1 Materials

$\text{Co}(\text{NO}_3)_2\cdot 6\text{H}_2\text{O}$ (>98.5%), ammonia (25wt%), KOH (>85wt%), NH_4NO_3 (>98%) all were analytical reagent and purchased from Tianjin Kermel Chemical Reagent Co. Ltd.

2.2 Samples Synthesis

Sample A was prepared as follow: 0.582 g of $\text{Co}(\text{NO}_3)_2\cdot 6\text{H}_2\text{O}$ was added into the pH=10.08 buffer solution which mixed by 2.5 mL of deionized water, 2.5 mL of ammonia and the appropriate amount of NH_4NO_3 . With 2h magnetic stirred continuously, the mixture color changed from orange to purple gradually with precipitating. Then 10 mL ethanol was added in order to precipitate completely.

After 2 h, the product was filtered, washed with ethanol and dried at 60 °C, successively. Finally it was heated with a ramp of 5 °C / min at nitrogen atmosphere in the tube furnace, 200 °C for 2 h and 600 °C for 4 h, respectively.

The sample B, C, D were prepared by following same process of sample A by changing buffer solution pH =9.90, 9.75 and 9.64 instead of 10.08, respectively.

2.3 Characterization

The phase identification of the sample was performed with a Bruker D8-advance X-ray powder diffractometer (Germany) equipped with Cu K radiation (40 kV, 40 mA), and with a scanning speed of 10° / min. The morphology of the products were recorded on Phenom ProX Scanning electron microscopy (Holland). X-ray photoelectron spectroscopy (XPS) analysis was obtained by Thermofisher K-alpha (USA).

2.4 Electrochemical properties

The working electrode was prepared as follow: according to the prepared sample, acetylene black and polytetrafluoroethylene weight ratio of 80 : 15 : 5, the mixture was pressed into the foamed nickel collector (1 cm²) under a pressure 10 MPa, and dried at 60 °C for 12 h. The loading mass of sample A, B, C and D were 2.6, 3.5, 3.6 and 3.2 mg, respectively. Prior to the test, the working electrode was immersed in a solution of 6 mol·L⁻¹ KOH in a vacuum environment for 24 h at room temperature.

Cycle voltammetry (CV), electrochemical impedance spectroscopy (EIS)(100 kHz to 0.01 Hz) and Galvanostatic charge-discharge test were performed by using GAMRY Reference1000 (USA) electrochemical workstation in a 6 mol·L⁻¹ KOH aqueous electrolyte at ambient temperature, with a standard three-electrode system containing a platinum foil counter electrode and a saturated calomel reference electrode.

The specific capacitance value of the sample were calculated according to the discharge time by using the formula: $C_s = I\Delta t / m\Delta V$. Where I is the constant discharge current (A), Δt is the discharge time (s), m is the cobalt oxides mass (g) of the electrode material on Ni collector, and ΔV is the potential window (V). The voltage range is 0 to 0.35 V.

3. RESULTS AND DISCUSSION

3.1 Characterization of samples

XRD patterns of the samples are shown in Fig.1. The diffraction peaks at 31.4 °, 36.6 °, 38.1 °, 44.3 °, 55.7 °, 59.8 ° and 65.1 ° can be respectively denoted as (220), (311), (222), (400), (422), (511) and (440) of cubic phase Co₃O₄ (JCPDS NO.43-1003). The peaks positioned at 36.3 °, 41.9 °, 61.5 ° and 74.8 ° in patterns belong to cubic phase CoO (JCPDS NO.43-1004). The variations

of (220) at 31.4° indicates that the crystallinity of Co_3O_4 in sample C is the worst.

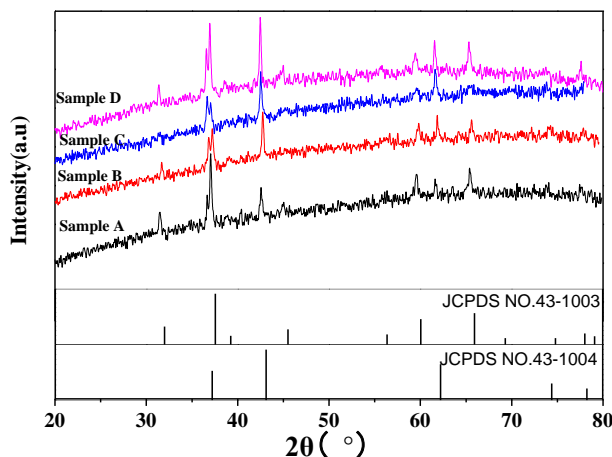


Figure 1. XRD spectrums of sample A (pH=10.08), sample B (pH=9.90), sample C (pH=9.75), sample D (pH=9.64)

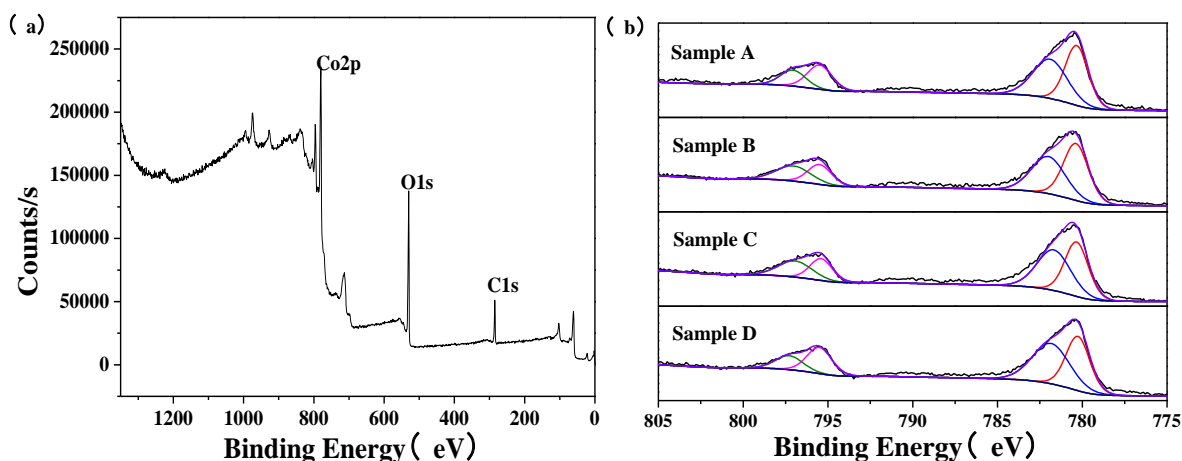
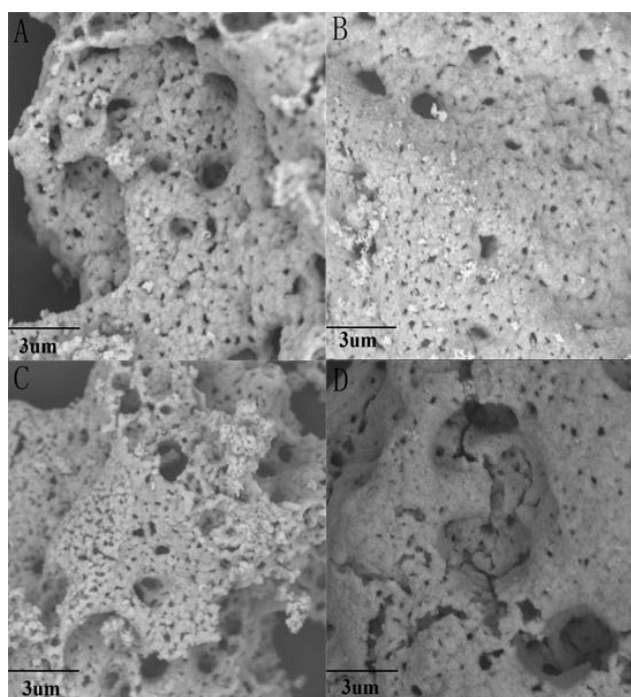


Figure 2. XPS spectrums (a) the full-survey-scan spectra of sample B and (b) the $\text{Co}2p$ XPS spectrum of the samples

The chemical bonding states of the materials was examined by XPS. Processing the data and dividing the peaks by Avantage v5, 52. As shown in Fig.2 (a), it indicates the presence of Co, O as well as C which is same as it from the reference. In the Fig.2 (b), the $\text{Co}2p$ XPS spectrum of the samples, a couple of peaks are present in both of $\text{Co}2p_{3/2}$ (781.28 eV / 779.58 eV) and $\text{Co}2p_{1/2}$ (796.18 eV / 794.78 eV), which are fitted with Co^{2+} and Co^{3+} of cobalt oxides, respectively. The content of the two valence states cobalt elements can be obtained by calculating the area of the dividing peaks. The content of Co (III) in samples are shown in Tab.1. From Tab.1, the content of Co (III) in all prepared samples are lower than that of pure Co_3O_4 (67%). Therefore, the results of XRD and XPS proved that the prepared samples are Co_3O_4 and CoO mixing together. Moreover, the content of Co (III) in sample C is lower than that of Co (II), which is consistent with the XRD results.

Table 1. The specific capacitance and content of Co^{3+}

Sample	A	B	C	D
Co (III) content (%)	53	52	49	51
Specific capacitance ($\text{F}\cdot\text{g}^{-1}$)	662.3	726.0	643.4	516.3

**Figure 3.** The SEM images of the samples at the same magnification

The morphology of the samples is investigated by SEM, as shown in Fig.3. The morphology shows that the cobalt oxides are honeycomb-like. The particles in the sample A, sample B and sample C are obviously different with different pore sizes. Sample A and sample C have more pores in the micron-scale than sample B. And sample B has the most uniform structure. In sample D, it is difficult to see its grain morphology. The uniform degree is sample B > sample A > sample C > sample D.

3.2 Electrochemical properties of the samples

The electrochemical performance of the samples with different working electrodes, was investigated in a three electrode systems with $6 \text{ mol}\cdot\text{L}^{-1}$ KOH aqueous electrolyte. Fig. 4 shows the cyclic voltammetry (CV) curves with a voltage window of 0 - 0.35 V for the samples evaluating rate of $5 \text{ mV}\cdot\text{s}^{-1}$. According to the previous reports, the specific capacitance is proportional to the integral area of the CV curves. Evidently, the area surrounded by the CV curve of the sample B is the largest. This result suggests that sample B has a better cyclic voltammetry performance. The CV curve shows the particular shape of all the samples with a pair of redox peaks (the peak at about 0.22 V is an

oxidation peak, which is a transition between $\text{Co}^{3+}/\text{Co}^{4+}$. A peak at about 0.1 V is a reduction peak of $\text{Co}^{3+}/\text{Co}^{2+}$, which were distinguished from the ideal rectangular shape of the EDLCs. Compared with the literature data [22], the redox peaks (especially the oxidation peak) were more perfect. This indicates that the reactions of the samples were more thorough. There was no polarization phenomenon and the potential difference between the oxidation peak and the reduction peak is about 0.1 V, which is smaller than that from literatures [23], indicating that the samples have excellent reversibility. Hence, the prepared samples were expected to be the ideal electrode materials. A pair of well-defined redox peaks appeared between 0 - 0.35 V in the CV curve, which is attributed to the two successive reactions as follows [22-25]:

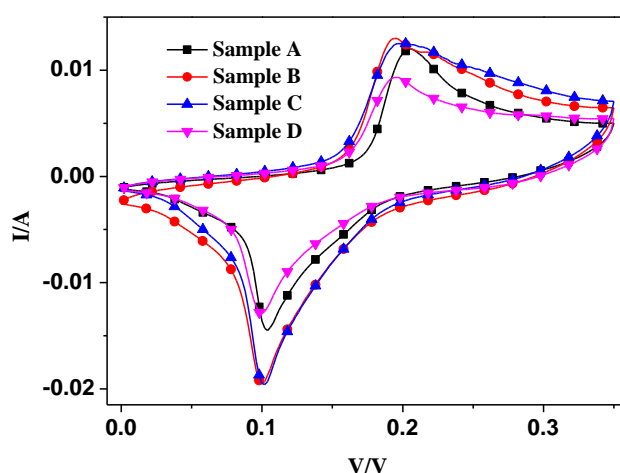
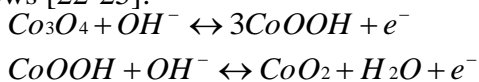


Figure 4. The cyclic voltammety curves of the samples at a scan rate of 5 mV s^{-1}

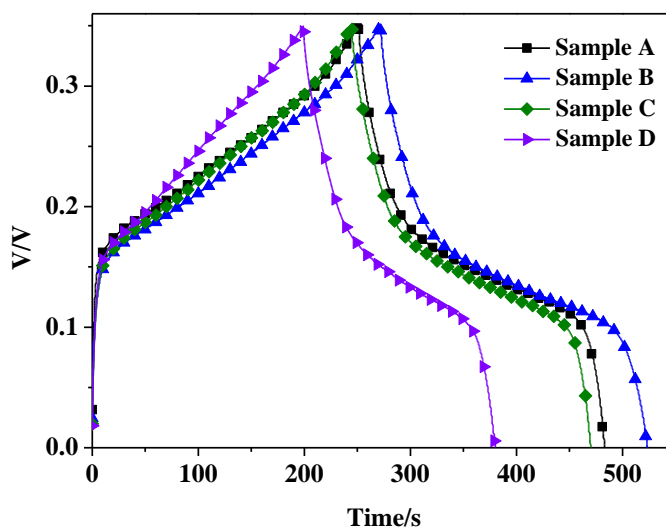


Figure 5. Charge and discharge curves for the samples at $1 \text{ A}\cdot\text{g}^{-1}$ current density

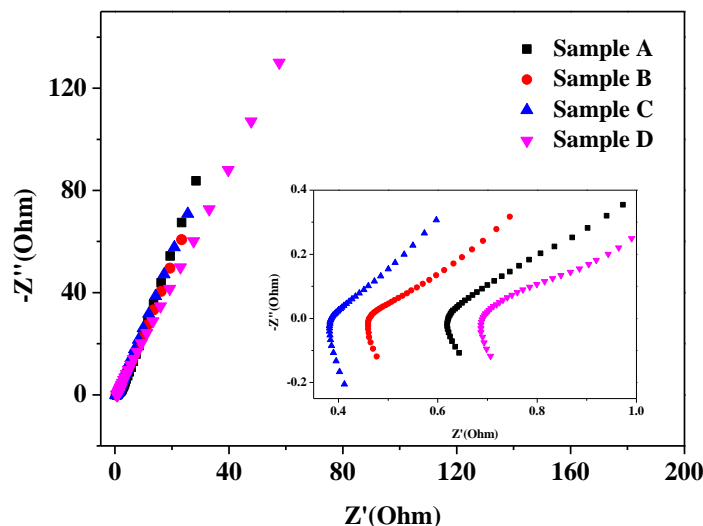
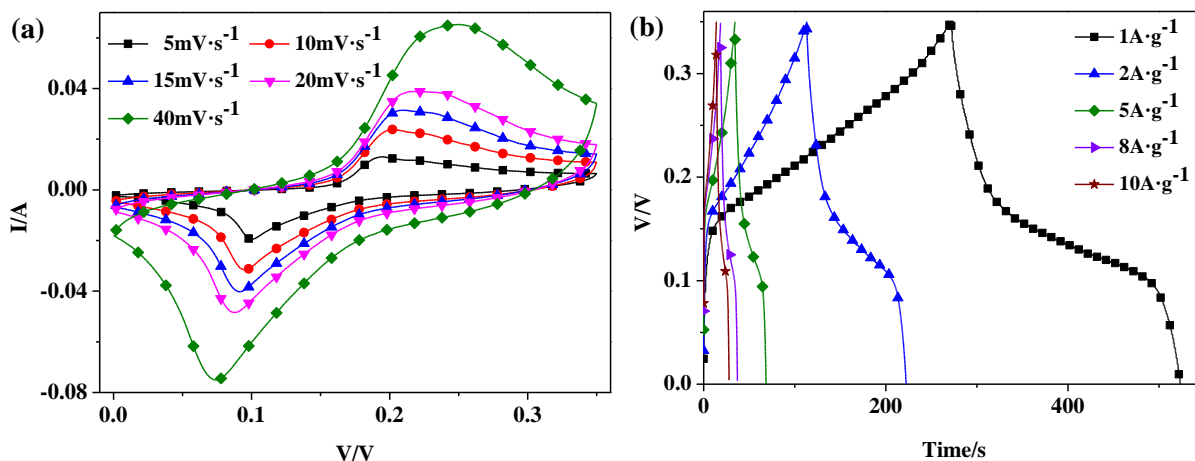


Figure 6. The EIS spectrum of samples

Fig.5 illustrates the galvanostatic charge-discharge curves of the samples at a current density of $1 \text{ A}\cdot\text{g}^{-1}$. The charge and discharge plateaus of curves indicate typical pseudo capacitance behavior of samples. The specific capacitances are sample B > sample A > sample C > sample D (shown in Tab.1). Sample D has the smallest specific capacitance due to it's the worst uniform degree. Sample C has smaller specific capacitance than sample B because the content of Co (III) is less than sample B. Compared with sample A which has a better uniform degree, sample B has the longest discharge time and the maximal specific capacitance, which indicates its excellent energy storage ability. This is consistent with the result of cyclic voltammetry test.

Electrochemical impedance spectroscopies (EIS) analysis was measured and the corresponding Nyquist plots are shown in Fig.6. In Fig.6, an enlarged view of the high frequency area was observed. As can be seen from the Fig.6, the internal resistances of the samples are all less than 1Ω , which shows the excellent conductivity of the prepared samples .



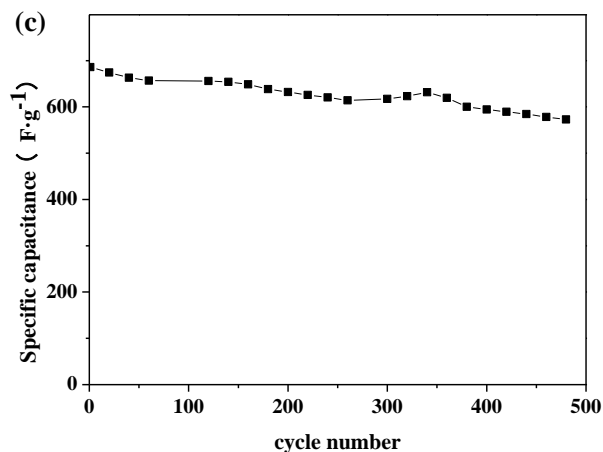


Figure 7. The cyclic voltammetry curves at different scan rates (a), charge and discharge curves at different current density (b) and the specific capacitance chart at 1 A g⁻¹(c) for sample B

Fig.7 (a) shows the CV curves of sample B at different scan rates of 5, 10, 15, 20, 40 mV·s⁻¹ which indicates that the reversibility of the sample B is excellent. The galvanostatic charge-discharge curves of sample B at different current density were performed as shown in Fig.7 (b). With density increasing from 1 A·g⁻¹ to 10 A·g⁻¹, the specific capacitance decreases from 726 F·g⁻¹ to 396.57 F·g⁻¹. The capacitance retention rate is 55%, demonstrating its excellent rate capability. The cycling stability of the the sample B by repeating charging-discharging processes was presented in Fig.7 (c). The capacitance retention is up to 83.5% after 500 cycles.

3.3 Mechanism analysis

Different from the literatures [15,16] which oxidized the Co (II) to Co (III) in the heat treatment process, the method were improved by adding NH₃-NH₄⁺ buffer solution into the solution of Co²⁺ salts to form [Co(NH₃)₆]²⁺, and Co (III) was obtained in the precursor formation process. Compared with literatures[17-20], as mentioned in the introduction, this method can ensure a stable pH and this may lead to less difference for the oxidation degree between the sample surface and internal. Summary of the above, there are two factors which affect the electrochemical properties of the cobalt oxides: the content of Co (III) and the uniform degree of the sample. Both these two factors depend on the control of the conditions in the precursor preparation process. The effect of pH on the content of Co (III) and the uniform degree of the sample can be explained by the effect of the acid-base balance, the redox balance, coordination balance and precipitation balance.

The concentration of NH₃ and OH⁻ in the solution is different due to the different pH of the buffer. Less concentration of NH₃ and OH⁻ when the buffer pH is low, the formation of [Co(NH₃)₆]²⁺ and Co(OH)₂ were competitive[26]. And when pH of the buffer rise, the content of NH₃ increase gradually. The formation of [Co(NH₃)₆]²⁺ is the dominant reaction and the probability of [Co(NH₃)₆]³⁺ conversion becomes larger[27,28]. So the content of Co (III) in the sample will increase. With the lowest content of Co (III), sample C has a poorer specific capacitance.

In addition, the higher the pH of the buffer is, the higher the hydroxyl content of the precursor becomes, and the calcination process can take off more water, which producing more micropores in the sample. Uniform pore structure is beneficial to improve the electrochemical properties. With the worst uniform degree, sample D has the worst electrochemical performance.

As sample A has a lower uniform degree, sample B has the maximal specific capacitance, which indicate its best energy storage ability.

4. CONCLUSION

The honeycomb-like cobalt oxides materials were prepared at pH=10.08, 9.90, 9.75, 9.64 for 2 h and then calcined for 4 h under 600 °C in a nitrogen atmosphere in the tube furnace. All the results indicate that the sample B has the best electrochemical performance. When the current density of samples increases from 1 A·g⁻¹ to 10 A·g⁻¹, the specific capacitance decreases from 726 F·g⁻¹ to 396.57 F·g⁻¹ with the capacitance retention rate of 55%. After 500 cycles charge and discharge at 1 A·g⁻¹, the retention rate is up to 83.5%. And the internal resistance of the material is less than 1 Ω. It indicated that the sample has good electrochemical performance and structural stability. Therefore, the prepared cobalt oxide materials has a good application prospect in the supercapacitor electrodes.

ACKNOWLEDGEMENTS

I would like to thank the Natural Science Foundation of Hebei Province (Nos. B2014201024) funding.

References

1. Q. Ke, C. Tang, Z. Yang, M. Zheng, L. Mao, H. Liu, J. Wang, *Electrochim. Acta*, 163 (2015) 9.
2. M. Kumar, A. Subramania, K. Balakrishnan, *Electrochim. Acta*, 149 (2014) 152.
3. C. Cheng, H. Fan, *Nano Today*, 7 (2012) 327.
4. J. Kang, A. Hirata, L. Kang, X. Zhang, Y. Hou, L. Chen, C. Li, T. Fujita, K. Akagi, M. Chen, *Angew. Chem. Int. Ed.*, 52 (2013) 1664.
5. S. Kuwabata, S. Masui, H. Tomiyori, H. Yoneyama, *Electrochim. Acta*, 46 (2000) 91.
6. Y. Xiao, S. Liu, F. Li, A. Zhang, J. Zhao, S. Fang, D. Jia, *Adv. Funct. Mater.*, 22 (2012) 4052.
7. J. Mu, B. Chen, Z. Guo, M. Zhang, Z. Zhang, P. Zhang, C. Shao, Y. Liu, *Nanoscale*, 3 (2011) 5034.
8. D. Liu, X. Wang, X. Wang, W. Tian, J. Liu, C. Zhi, D. He, Y. Bando, D. Golberg, *J. Mater. Chem. A*, 1 (2013) 1952.
9. X. Zhang, W. Shi, J. Zhu, W. Zhao, J. Ma, S. Mhaisalkar, T. Maria, Y. Yang, H. Zhang, H. Hng, Q. Yan, *Nano Res.*, 3 (2010) 643.
10. S. Kim, J. Lee, H. Ahn, H. Song, J. Jang, *ACS Appl. Mater. Interfaces*, 5 (2013) 1596.
11. J. Kwak, Y. Lee, J. Bang, *Mater. Lett.*, 110 (2013) 237.
12. K. Qiu, H. Yan, D. Zhang, Y. Lu, J. Cheng, W. Zhao, C. Wang, Y. Zhang, X. Liu, C. Cheng, Y. Luo, *Electrochim. Acta*, 141 (2014) 248.
13. J. Zhao, P. Liu, W. Zhang, B. Tang, J. Xu, *Journal of Shanghai University of Engineering Science*, 24 (2010) 262.
14. Y. Fan, G. Shao, Z. Ma, G. Wang, H. Shao, S. Yan, *Part. Part. Syst. Char.*, 31 (2014) 1079.
15. D. Wang, Q. Wang, T. Wang, *Inorg. Chem.*, 50 (2011) 6482.
16. Y. Zhang, Z. Song, W. Liu, M. Lei, *Power Technol.*, 38 (2014) 1875.
17. H. Lu, J. Yan, Y. Zhang, Y. Huang, W. Gao, W. Fan, T. Liu, *ChemNanoMat*, 2 (2016) 972.
18. J. Liu, *Harbin Engineering University*, 2011.
19. T. Nguyen, V. Nguyen, R. Deivasigamani, D. Kharismadewi, Y. Iwai, J. Shim, *Solid State Sci.*, 53

- (2016) 71.
20. S. Wang, Q. Li, M. Chen, W. Pu, Y. Wu, M. Yang, *Electrochim. Acta*, 215 (2016) 473.
 21. J. Dean, *Lange's handbook of chemistry*, (1972) 846.
 22. X. Deng, J. Li, S. Zhu, F. He, C. He, E. Liu, C. Shi, Q. Li, N. Zhao, *J. Alloys Compd.*, 693 (2017) 16.
 23. W. Bao, B. Yu, W. Li, H. Fan, J. Bai, Z. Ren, *J. Alloys Compd.*, 647 (2015) 873.
 24. H. Fan, L. Quan, M. Yuan, S. Zhu, K. Wang, Y. Zhong, L. Chang, H. Shao, J. Wang, J. Zhang, C. Cao, *Electrochim. Acta*, 188 (2016) 222.
 25. X. Ge, C. Gu, X. Wang, J. Tu, *J. Phys. Chem. C*, 118 (2014) 911.
 26. Z. Ma, Z. Li, G. Zhou, G. Jia, *Inorganic and Analytical Chemistry*, Chemical Industry Press, 2014.
 27. X. Liu, Y. Zhu, F. Gao, *Inorganic Element Chemistry*, Science Press, 2010.
 28. G. Wu, *Inorganic Chemistry*, Higher Education Press, 2003.

© 2018 The Authors. Published by ESG (www.electrochemsci.org). This article is an open access article distributed under the terms and conditions of the Creative Commons Attribution license (<http://creativecommons.org/licenses/by/4.0/>).